Direct Path Interference Suppression Requirements for Bistatic Backscatter Communication System

Ritayan Biswas*, Muhammad Usman Sheikh†, Hüseyin Yiğitler†, Jukka Lempiäinen*, and Riku Jäntti†
*Laboratory of Electronics and Communications Engineering, Tampere University, 33720 Tampere, Finland
Email: {ritayan.biswas, jukka.lempiainen}@tuni.fi
†Department of Communications and Networking, Aalto University, 02150 Espoo, Finland.
Email: {muhammad.sheikh, yusein.ali, riku.jantti}@aalto.fi

***Abstract*—The ambient backscatter communication (AmBC) system utilizes the existing ambient RF signals present in the atmosphere for backscattering the signal. One of the challenges for AmBC system is the interference at the receiver module caused by the direct path signal from the ambient source. The purpose of this paper is to study the coverage aspects of the bi-static backscatter communication system in a typical urban environment at sub-1GHz frequencies using simulations in MATLAB. For the simulation, 3rd generation partnership project (3GPP) urban microcellular and international telecommunication union (ITU) device-to-device (D2D) propagation models are used. Moreover, the dynamic range i.e., the difference in the received power level of the direct path and the backscatter path is investigated. For correctly decoding the backscatter signal at the reader, the target value set for the dynamic range is less than 30 dB. This paper studies the importance of direct path interference suppression for the successful deployment of a bi-static backscatter communication system.**

***Index Terms*—IoT, Backscatter communications, AmBC, Dynamic range, Interference suppression**

I. Introduction

The Internet of things (IoT) is a wireless communication paradigm where sensors are utilised to collect and process the information from the environment [1], and for sending the data for post processing. IoT is considered as a key enabling technology for the future wireless technologies i.e., for fifth generation (5G) and beyond. IoT has various applications in our daily lives e.g., the IoT sensors can be used to measure the temperature, humidity, air pollution, car traffic density, health related parameters, agriculture, for counting the objects, and for detecting different events [1].

Low power wide area networks (LPWAN) such as long range (LoRa) radio, Sigfox and narrow band IoT (NB-IoT) have been proposed as key enabling technologies for the practical deployment of IoT in real life cases [2]. These technologies are designed to provide wide coverage for a large number of sensors simultaneously. Additionally, these technologies incur low costs and consume low energy. Due to the variety of use cases, IoT sensors are expected to be deployed in huge numbers and at a variety of locations, especially in the urban environment. Although, there are certain advantages of the aforementioned LPWAN technologies, the major drawback associated with these technologies is the energy consumption, and the need for a dedicated transmission signal [3].

Backscatter communication (BC) is a technology where an IoT sensor i.e., in this case called a backscatter device (BD) receives the incoming RF signal from the transmitter (Tx) antenna, modulates and forwards it to the receiver also known as reader [3]. In case of the ambient BC (AmBC), the radio signal generated by a non-dedicated transmitter is reflected back from a BD to the reader. In AmBC, the BDs can operate in a passive or semi-passive mode. In semi-passive mode, the BDs are capable of harvesting the energy from the cellular networks, television broadcasts and from WiFi signals to name a few. Therefore, AmBC is a step towards battery free and the wireless operation of the sensors [3].

The authors in [4] were the first to introduce the concept of AmBC by utilising the ambient television broadcast signal in the year 2013. They were able to achieve an AmBC link for a short range. The link budgets for different modes of backscatter systems were presented in references [5], [6]. Although the maturing of the technology has helped in achieving improvements over traditional backscatter systems. The performance of the BC system is limited by the short communication ranges and low data rates. This is due to the direct path interference and weak backscatter signal, since these two signals are summed at the receiver. Therefore, the limitations of BC must be investigated to identify the bottlenecks and check the feasibility of the technology for application specific scenarios. In this work, considering a legacy cellular system, first the power difference between the direct path and backscatter signal is computed, then the required amount of direct path signal suppression requirement is found, prior to the analog-to-digital conversion of the composite signal. Although this work is not limited on a specific type of direct path signal suppression method, a realistic assumption about the receiver hardware is made, where the signal power difference is lower than a threshold so that digital processing can be successfully applied.

II. Backscatter communication

A. Asymbiotic Backscatter Communications

The two major variants of the asymbiotic backscatter technology are the mono-static and bi-static backscatter. In the mono-static backscatter, the Tx antenna and the receiver module are essentially the same device. Thus, the signal propagates from the Tx antenna and reflects back at the receiver module from the sensor. Radio frequency identification (RFID) is an example of mono-static backscatter technology. The Tx antenna and the receiver module are located away from each other while operating in the bi-static backscatter mode of operation. The signal from the Tx antenna is forwarded to the receiver terminal after reflection from the sensor. A major drawback of an asymbiotic backscatter system is the need to generate a dedicated signal.

B. Symbiotic (Ambient) Backscatter Communications

Ambient backscatter communication is a symbiotic wireless communication technique where the signals from ambient RF sources are conveyed forward by BDs, without needing active RF components. Generally, the frequency of operation of the backscatter signal is the same as that of the incoming signal source and utilises the same spectrum [7]. However, it is stated in [3] that frequency of the backscatter signal can be shifted to the adjacent non-overlapping frequency band for robust decoding. AmBC promises to provide high spectral and energy efficiency [7]. There are numerous sources of ambient RF signals such as television broadcasts, WLAN signals and cellular signals. Furthermore, as no external power source is utilised, AmBC is a green technology having a very low environmental footprint.

The schematic diagram of the bi-static backscatter system is illustrated in Fig. 1. AmBC has several advantages over the traditional BC system. The backscatter signal has much lower amplitude compared with the legacy system's signal i.e., the direct path. The receiver decodes the backscatter signal that impinges at the receiver antenna together with the legacy systems' direct path signal. The receiver design for these systems is challenging. In particular, if the direct path is not suppressed in the analog domain before the automatic gain control (AGC) unit and the analog-to-digital converter (ADC) the numerical values of the digital signal are dominated by the legacy system signal, and the backscatter signal is pushed toward the least significant bits. For example, if the receiver effectively has 12-bits of resolution (here, one may include the number of AGC gain steps into the resolution), the AGC loop would adjust its gain so that the largest amplitude is quantized into the approximately 10^{th} bit, and the average signal approximately into the 6^{th} bit. As a consequence, when the amplitude difference between these two signals exceeds $30\,\mathrm{dB}$, the backscatter signal would be only be represented in the least significant bit of the ADC output. Such a low SNR operation easily reaches the SNR wall of the signal detection [8], which makes digital signal processing techniques ineffective. Therefore, studying direct path interference requirements for backscattering receivers is a fundamental problem and must be addressed for each deployment.

The dynamic range of the system is defined by the difference in the signal strength of the strongest (legacy) and the weakest (backscatter) signal. In order to improve the range and/or data rate of the backscatter system, the receiver must be able to handle the large difference between these two signals. The easiest solution is to increase the receiver resolution, which is costly for high-speed systems. The other solutions include analog domain suppression techniques, which requires to exploit certain differences between these two signals. In case of shifting the signal to another band by the BD [3], analog filtering can be used. Whereas, for a receiver with multiple antennas, directional difference can be used [9]. Finally, if two systems are able to work on differently polarized signals, their polarization differences can be used for suppressing the legacy system signal [10]. Regardless of the adopted technique, the power difference of these signals should be investigated for deployment before selecting the suppression technique.

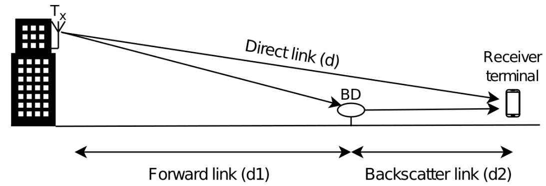

Fig. 1. Schematic diagram of the propagation environment.

III. Propagation models

A. 3GPP - Urban microcellular model

The 3GPP has developed a propagation model operating at different frequencies in an urban microcellular environment [11]. This model is valid for the scenarios where the Tx antennas are mounted below the rooftops ($10\,\mathrm{m}$ to $15\,\mathrm{m}$) of surrounding buildings. The basic path loss in line of sight (LOS) and non-LOS (NLOS) condition is computed by using eq. 1 and eq. 2, respectively.

$$L_{\mathrm{LOS}}(\mathrm{dB}) = 32.4 + 20 \cdot \log_{10}(f_{\mathrm{GHz}}) + 21 \cdot \log_{10}(d_{\mathrm{3D}}), \quad (1)$$

$$L_{\mathrm{NLOS}}(\mathrm{dB}) = 32.4 + 20 \cdot \log_{10}(f_{\mathrm{GHz}}) + 31.9 \cdot \log_{10}(d_{\mathrm{3D}}). \quad (2)$$

where the term d_{3D} is expressed in meters and represents the direct path followed by the signal (to the BD). The frequency of the signal is expressed in GHz, and subsequently, the LOS probability is calculated using eq. 3,

$$P_{\mathrm{LOS}} = \begin{cases} 1, & d_{\mathrm{2D}} \leq 18m \\ \dfrac{18}{d_{\mathrm{2D}}} + \left(-\dfrac{d_{\mathrm{2D}}}{36}\right)\left(1 - \dfrac{18}{d_{\mathrm{2D}}}\right), & 18m < d_{\mathrm{2D}} \end{cases} \quad (3)$$

where the term d_{2D} represents the distance between the T_{x} antenna and the BD in meters. Therefore, d_{2D} is the base of the triangle formed by the antenna, the ground and the sensor. The term d_{3D} represents the hypotenuse of this triangle. The total loss in the forward link (L_{d1}) is computed using eq. 4,

$$L_{\mathrm{d1}} = P_{\mathrm{LOS}} \times L_{\mathrm{LOS}} + (1 - P_{\mathrm{LOS}}) \times L_{\mathrm{NLOS}}, \quad (4)$$

B. ITU - Device to device (D2D) model

International telecommunication union (ITU) specifies a model for communication between two devices located in an urban microcellular street canyon environment [12]. The model calculates the basic transmission loss while taking into account the location variability statistics for the LOS and the NLOS regions [12]. The calculation of the LOS basic transmission loss is performed by using eq. 5,

$$L_{\text{LOS}}(d) = 32.45 + 20 \cdot \log_{10}(f_{\text{MHz}}) + 20 \cdot \log_{10}(d_{\text{3D}}), \quad (5)$$

where f_{MHz} is the frequency expressed in MHz and the distance (d_{3D}) is expressed in meters. Subsequently, the LOS location correction is computed for the required location percentage (p) by using eq. 6,

$$\Delta L_{\text{LOS}}(p) = 1.5624\sigma(\sqrt{-2 \cdot ln(1 - p/100)} - 1.1774). \quad (6)$$

Subsequently, the LOS location correction ($\Delta L_{\text{LOS}}(p)$) is added to the median value of the LOS basic transmission loss ($L_{\text{LOS}}(d)$) using eq. 7,

$$L_{\text{LOS}}(d, p) = L_{\text{LOS}}(d) + \Delta L_{\text{LOS}}(p). \quad (7)$$

The NLOS basic transmission loss is computed using eq. 8, where the frequency is expressed in MHz and the distance in meters. The value of L_{urban} is $6.8\,\text{dB}$ and is indicative of the type of urban environment [12]. The NLOS location correction is computed for the required location percentage using eq. 9,

$$L_{\text{NLOS}}(d) = 9.5 + 45 \cdot \log_{10}(f_{\text{MHz}}) + 40 \cdot \log_{10}(d_{\text{3D}}) + L_{\text{urban}}, \quad (8)$$

$$\Delta L_{\text{NLOS}}(p) = \sigma \cdot N^{-1}(\frac{p}{100}), \quad (9)$$

where $N^{-1}(.)$ is the inverse normal cumulative distribution function. Subsequently, the NLOS location correction (ΔL_{NLOS}) is added to the median value of the NLOS basic transmission loss $L_{\text{NLOS}}(d)$ to obtain the total NLOS loss using eq. 10,

$$L_{\text{NLOS}}(d, p) = L_{\text{NLOS}}(d) + \Delta L_{\text{NLOS}}(p). \quad (10)$$

Furthermore, the corner distance, d_{LOS} is calculated as a function of the location percentage p and is calculated using eq. 11,

$$d_{\text{LOS}}(p) = \begin{cases} 212 \cdot [\log_{10}(\frac{p}{100})]^2 - 64 \cdot \log_{10}(\frac{p}{100}), & p < 45 \\ 79.2 - 70 \cdot (\frac{p}{100}), & 45 \leq p \end{cases} \quad (11)$$

Finally, the total loss in the backscatter link (L_{d2}) is computed utilising the criteria stated in eq. 12, taking into account the loss in the LOS and NLOS regions,

$$L_{\text{d2}} = \begin{cases} L_{\text{LOS}}(d, p), & d < d_{\text{LOS}} \\ L_{\text{NLOS}}(d, p), & d > d_{\text{LOS}} \end{cases} \quad (12)$$

IV. Simulation setup and parameters

A schematic diagram of the propagation environment is shown in Fig. 1. The propagation for bi-static AmBC is a combination of two links. The first link ($d1$, forward link) is the connection between the T_{x} antenna and the sensor. The second link ($d1$, backscatter link) is the connection between the sensor and the receiver equipment. In this work, the definition of the forward link is provided by 3GPP and the backscatter link for communication between two devices is defined by the ITU. The simulations are performed in an environment depicting an urban street canyon. The transmit power ($P_{T_{\text{x}}}$) of the T_{x} antenna in such an environment is $2\,\text{W}$ i.e., $33\,\text{dBm}$. Typical cellular frequencies operating at less than $1\,\text{GHz}$ are utilised for the simulations. The received power level is calculated using eq. 13.

TABLE I
Simulation parameters.

Parameters	Unit	Value
Frequency	MHz	200/500/700/900
T_{x} power	dBm	33
T_{x} antenna height	m	15
T_{x} antenna gain	dBi	10
BD antenna gain	dBi	0
Slow fading margin	dB	15.2
Fast fading margin	dB	16
Polarization mismatch loss	dB	3
Modulation loss	dB	6
L_{urban}	dB	6.8
Location percentage	%	50

$$RX_{\text{level}}(\text{dBm}) = P_{\text{tx}} + G_{\text{t}} - (L_{\text{d1}} + L_{\text{d2}} + L_{\text{add}}), \quad (13)$$

where L_{d1} and L_{d2} is the basic transmission loss in the forward and the backscatter link, respectively. G_{t} represents the gain of the T_{x} antenna. The additional losses (L_{add}) in the communication link is contributed by the slow fading (L_{SF}), fast fading (L_{FF}), polarization mismatch (L_{PM}) and modulation loss (L_{ML}) and is calculated using eq. 14,

$$L_{\text{add}} = L_{\text{SF}} + L_{\text{FF}} + L_{\text{PM}} + L_{\text{ML}} \quad (14)$$

The reference values of the aforementioned losses and margins are obtained from [6] where a complete link budget is provided for backscatter systems. The values of these parameters are summarised in Table I, and are used for the simulation work of this paper.

V. Results and Analysis

Fig. 2(a-d) shows the received signal level at the receiver i.e., reader, for different combinations of the forward and the backscatter link distances at four different sub-GHz frequencies. The target is to determine the feasibility of the received power with respect to the receivers' sensitivity of typical IoT technologies such as the LoRa backscatter and NB-IoT. It is reported at references [13], [14] that the LoRa backscatter and NB-IoT have a receiver sensitivity of $-149\,\text{dBm}$ and $-141\,\text{dBm}$, respectively. Therefore, in the rest of our analysis these threshold values are used as a reference for coverage.

It can be seen in Fig. 2(a), that considering LoRa backscatter technology at $200\,\text{MHz}$ there is good coverage at considered distances in the forward and backscatter link. It was found that considering the LoRa receiver sensitivity level the reader should be able to hear the signal at $150\,\text{m}$ for the forward link and $60\,\text{m}$ for the backscatter link. Whereas, for NB-IoT, the coverage area is reduced to $115\,\text{m}$ and $60\,\text{m}$ for the forward and backscatter link, respectively. In other words the coverage

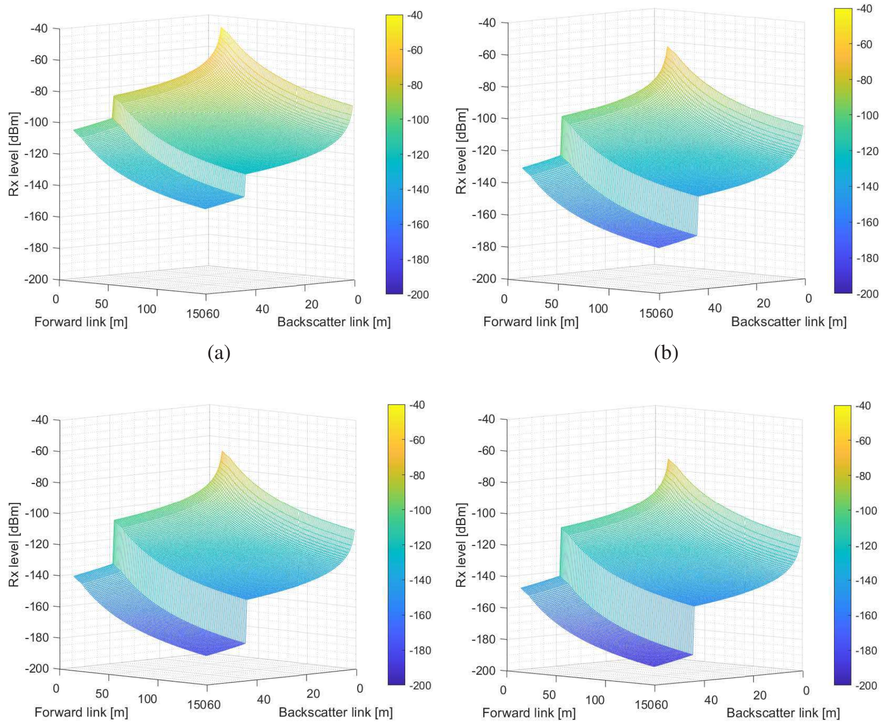

(a) (b) (c) (d)

Fig. 2. Received power level at the receiver at, (a) 200 MHz, (b) 500 MHz, (c) 700 MHz, and (d) 900 MHz.

in the forward link can be extended to $150\,\mathrm{m}$ for backscatter link upto $45\,\mathrm{m}$. It is observed from Fig. 2 that the signal strengths at the receiver decreases sharply when the receiver terminal is moved from the LOS to the NLOS region at all frequencies.

For higher frequencies i.e., for 500 MHz and 700 MHz, it can be observed in Fig. 2(b-c) that there is coverage in the LOS region when LoRa technology is considered. However, the coverage in the NLOS region is limited to short distances only. The maximum achievable distance is $62\,\mathrm{m}$ (forward link) and $44\,\mathrm{m}$ (backscatter link) at $500\,\mathrm{MHz}$. At $700\,\mathrm{MHz}$, the maximum achievable range in the NLOS region is $30\,\mathrm{m}$ in the forward link when the backscatter link is $60\,\mathrm{m}$. Similarly, for NB-IoT technology, the maximum range of communication in the NLOS region at $500\,\mathrm{MHz}$ is $42\,\mathrm{m}$ (forward link) and $44\,\mathrm{m}$ (backscatter link), and at $700\,\mathrm{MHz}$, the maximum range of communication in the NLOS range is $17\,\mathrm{m}$ in the forward link and $60\,\mathrm{m}$ in the backscatter link. From Fig. 2(d), it is clearly evident that the 900 MHz band is only feasible for short range communication and is unsuitable for long range IoT networks. These results shows the potential of using 200 MHz for IoT type of services, and signifies the importance of 200 MHz band for future smart city deployment, as long range coverage is a bottle neck even for technologies with very good receiver sensitivity level i.e., the LoRa backscatter and NB-IoT.

Fig. 3 shows the dynamic range of the bistatic backscatter system for four different considered frequencies. It can be observed from Fig. 3(a), that at the frequency of 200 MHz, the dynamic range of the signal varies between $14\,\mathrm{dB}$ and $47\,\mathrm{dB}$ in the LOS region. Whereas the dynamic range has values from $61.5\,\mathrm{dB}$ to $74\,\mathrm{dB}$ in the NLOS region. It is important to here re-call that in most of the practical AmBC systems the required dynamic range is below 30 dB as mentioned in the Section II-B, therefore the target is to achieve the dynamic range below the aforementioned threshold for correctly decoding the bits. By analyzing the results presented in Fig. 2(a) and Fig. 3(a) collectively, it can be said that at 200 MHz for IoT technologies like the LoRa backscatter and NB-IoT the limiting factor is not the coverage rather it is the dynamic range, and therefore interference suppression techniques mentioned in the Section II-B or any other means should be utilised to suppress the direct path. It is also revealed in Fig. 3(a-d) that the value of dynamic range increases with the increase in the frequency of operation, as in Fig. 3(b) the dynamic range has values between $22\,\mathrm{dB}$ and $55\,\mathrm{dB}$ in the LOS region, and similarly for other higher frequencies higher values of dynamic range were found.

VI. Conclusion

In this paper, we studied the coverage aspects of the bi-static BC mode at four targeted frequencies at sub-1GHz band in an urban microcellular environment through simulations. The received signal levels at the receiver were computed for different combinations of forward link and backscatter link distances, and it was found that at 200 MHz considering the LoRa receiver sensitivity level the reader should be able to

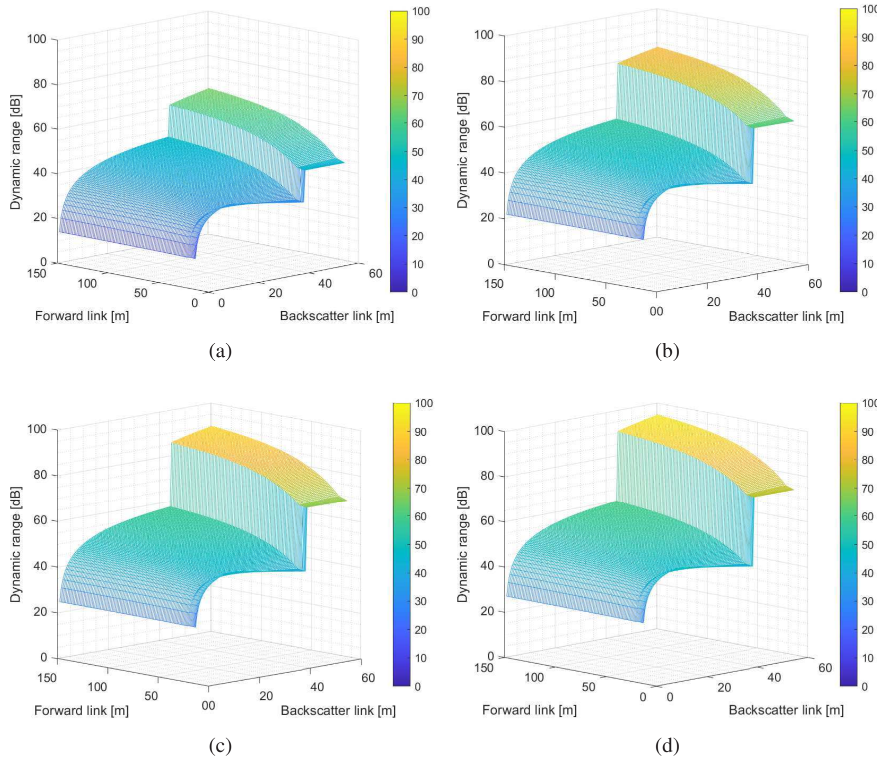

Fig. 3. Dynamic range at, (a) 200 MHz, (b) 500 MHz, (c) 700 MHz, and (d) 900 MHz.

hear the signal at $150\,\mathrm{m}$ for the forward link and $60\,\mathrm{m}$ for the backscatter link. Whereas, for NB-IoT signal technology, the coverage area shrinks to $115\,\mathrm{m}$ for the forward link and $60\,\mathrm{m}$ for the backscatter link. Even at 500 MHz it was hard to find long range coverage for both LoRa and NB-IoT in NLOS region. More interestingly, it was found that the limiting factor is not the coverage rather it is the dynamic range, as at 200 MHz frequency of operation for the considered distances the dynamic range of the signal varied between $14\,\mathrm{dB}$ and $47\,\mathrm{dB}$ in the LOS region, and in NLOS the value of dynamic range is even higher. These results signifies the importance of direct path interference suppression techniques, only migrating to a lower frequency band will not help in extending the coverage of the backscatter communication system unless the direct path interference is not properly mitigated.

References

[1] A. Al-Fuqaha, M. Guizani, M. Mohammadi, M. Aledhari, and M. Ayyash, "Internet of things: A survey on enabling technologies, protocols, and applications," *IEEE Communications Surveys Tutorials*, vol. 17, no. 4, pp. 2347–2376, 2015.

[2] W. Ayoub, A. E. Samhat, F. Nouvel, M. Mroue, and J. Prévotet, "Internet of mobile things: Overview of lorawan, dash7, and nb-iot in lpwans standards and supported mobility," *IEEE Communications Surveys Tutorials*, vol. 21, no. 2, pp. 1561–1581, 2019.

[3] N. Van Huynh, D. T. Hoang, X. Lu, D. Niyato, P. Wang, and D. I. Kim, "Ambient backscatter communications: A contemporary survey," *IEEE Communications Surveys Tutorials*, vol. 20, no. 4, pp. 2889–2922, 2018.

[4] V. Liu, A. Parks, V. Talla, S. Gollakota, D. Wetherall, and J. R. Smith, "Ambient backscatter: Wireless communication out of thin air," *SIGCOMM Comput. Commun. Rev.*, vol. 43, no. 4, pp. 39–50, Aug. 2013. [Online]. Available: http://doi.acm.org/10.1145/2534169.2486015

[5] M. U. Sheikh, R. Duan, and R. Jantti, "Validation of backscatter link budget simulations with measurements at 915 mhz and 2.4 ghz," in *2019 IEEE 89th Vehicular Technology Conference (VTC2019-Spring)*, 2019.

[6] J. D. Griffin and G. D. Durgin, "Complete link budgets for backscatter-radio and rfid systems," *IEEE Antennas and Propagation Magazine*, vol. 51, no. 2, pp. 11–25, April 2009.

[7] H. Guo, Y. Liang, R. Long, and Q. Zhang, "Cooperative ambient backscatter system: A symbiotic radio paradigm for passive iot," *IEEE Wireless Communications Letters*, vol. 8, no. 4, pp. 1191–1194, 2019.

[8] R. Tandra and A. Sahai, "Snr walls for signal detection," *IEEE Journal of Selected Topics in Signal Processing*, vol. 2, no. 1, pp. 4–17, 2008.

[9] R. Duan, E. Menta, H. Yigitler, R. Jantti, and Z. Han, "Hybrid beamformer design for high dynamic range ambient backscatter receivers," in *2019 IEEE International Conference on Communications Workshops (ICC Workshops)*, 2019, pp. 1–6.

[10] J. Lietzén, A. Liljemark, R. Duan, R. Jäntti, and V. Viikari, "Polarization conversion-based ambient backscatter system," *IEEE Access*, vol. 8, pp. 216 793–216 804, 2020.

[11] 3GPP, "Study on channel model for frequencies from 0.5 to 100 ghz," 3rd Generation Partnership Project (3GPP), Technical Report (TR) 38.901, 12 2017, version 14.3.0.

[12] ITU-R, "Propagation data and prediction methods for the planning of short-range outdoor radio communication systems and radio local area networks in the frequency range 300 mhz to 100 ghz," International Telecommunication Union (ITU), Recommendation ITU-R P.1411-10, 08 2009.

[13] V. Talla, M. Hessar, B. Kellogg, A. Najafi, J. R. Smith, and S. Gollakota, "LoRa backscatter: Enabling the vision of ubiquitous connectivity," in *Ubicomp*, Boston, MA, Mar. 2017, pp. 243–258.

[14] R. Ratasuk, N. Mangalvedhe, Y. Zhang, M. Robert, and J. Koskinen, "Overview of narrowband iot in lte rel-13," in *2016 IEEE Conference on Standards for Communications and Networking (CSCN)*, 2016, pp. 1–7.